Trends in metal–ligand orbital mixing in generic series of ruthenium N-donor ligand complexes— effect on electronic spectra and redox properties

S.I. Gorelsky, E.S. Dodsworth, A.B.P. Lever *, A.A. Vlcek

Department of Chemistry, York University, 4700 Keele Street, Toronto, Ont. M3J 1P3, Canada

Contents

Abstract

Generic series of complexes $[Ru(bpy)_{3-n}(LL)_n]^{2+}$ (bpy = 2,2'-bipyridine), where LL is a diimine ligand including specifically 2,2'-bipyrazine (bpz), 2,2'-azobipyridine (abpy), and *o*-benzoquinonediimine (bqdi), are studied with respect to their electrochemistry, optical spectroscopy and electronic structure as elucidated using Zerner's INDO/S method. Characteristics of their electrochemistry and optical spectroscopy are explained in terms of mixing between ruthenium d orbitals and diimine ligand π and π* orbitals, increasing in importance from bpy to bpz to abpy to bqdi. In this last case, these species have characteristics not unlike fully delocalized organic molecules. © 1998 Elsevier Science S.A. All rights reserved.

* Corresponding author. Tel: + 1 416 736 2100 ext. 22309; Fax: + 1 416 736 5936; E-mail: blever@yorku.ca

1. Introduction

In the past several years we have studied a number of systems, particularly ruthenium complexes containing strongly π-accepting quinonoid ligands [1–9] in which charge transfer (CT) bands, upon changing ligand substituent or co-ligand, sometimes shift in energy in the opposite direction to that expected on the basis of a simple model (vide infra Eq. (1)). We have been interested in the bonding in such species and in the cause of the shifts, particularly in terms of the amount of mixing occurring therein between metal d-orbitals and ligand π- or π*-orbitals. With the wider availability of computational methods that can be used for second-row transition metals we are now in a position to explain some of these data in terms of orbital mixing effects.

Recently, there have been several investigations focusing on the prediction of electronic spectra and identifying the extent of ruthenium–ligand electronic coupling in both mononuclear and dinuclear species from the laboratories of Zerner and co-workers [10], Hush and co-workers [11–14], Boxer and co-workers [15,16], Creutz and co-workers [17–20], Broo and Lincoln [21], Sizova and coworkers [22–26] and Clarke and co-workers [27] and mostly using INDO/S or variants thereof. In this paper we compare the series of complexes $[Ru(bpy)_{3-n}(bqdi)_n]^{2+}$, containing 2,2'-bipyridine (bpy) with the strongly π-accepting ligand o-benzoquinonediimine (bqdi), with similar series of complexes of bpy containing the weaker π-acceptors 2,2'-bipyrazine (bpz) and 2,2'-azobipyridine (abpy) (Fig. 1). These series are referred to as generic series.

As we demonstrate below, both the abpy and bqdi complexes show unusual behavior (explained below) when their first reduction potentials and the energies of their visible region spectroscopic transitions are considered through the series. A similar series of ruthenium(II) complexes containing bpy and orthometallated phenylpyridine has been studied by Fenske–Hall calculations and reported by Constable and Housecroft [28], though experimental data were not available for all the complexes. Aside from this last paper, this is the first detailed attempt to discuss the electronic coupling in ruthenium complexes containing several potentially π-accepting ligands and focusing on the interplay between these ligands. The consideration of trends in homologous series is a useful procedure for highlighting unusual behavior which may occur for specific members of such series. Haga et al. have also applied this method for some ruthenium species [29].

The subject of orbital mixing is relevant to the development of conducting polymers in which transition metals are part of the conducting backbone; for example [30,31] a novel conducting polymer contains an analogue of bqdi, para-benzoquinonediimine.

The bonding in transition metal complexes is usually described in terms of ionic and covalent interactions. The success of simple ligand field models is due to the fact that the bonding in complexes of first-row transition metals is primarily ionic, although even within the framework of ligand field theory covalent effects cannot be ignored and are included as the nephelauxetic effect [32]. We are concerned specifically with the question of whether, in these low spin Ru(II) species, the t_{2g}^6 electrons are localized solely on the ruthenium center, or are delocalized to a greater
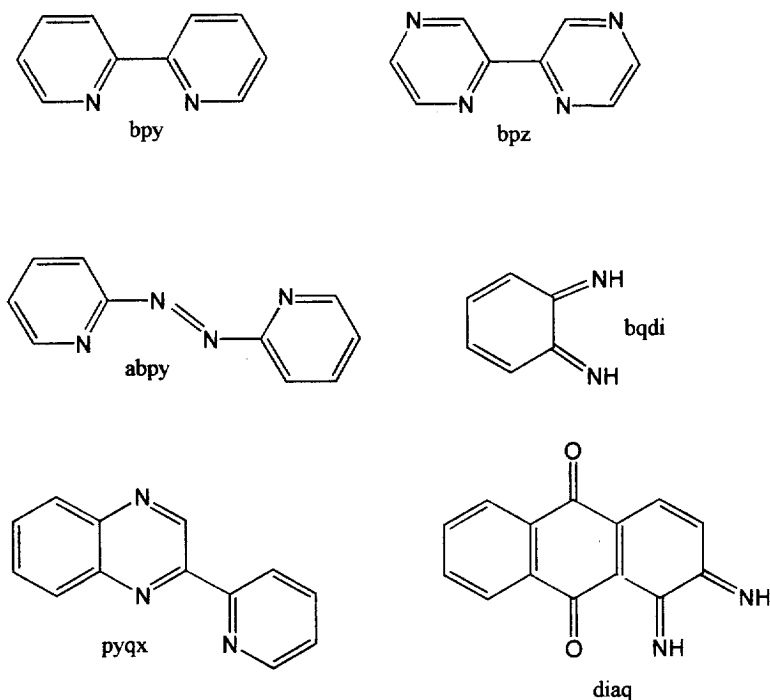
Fig. 1. Structures of the ligand discussed in this contribution.

or lesser degree on the diimine ligand due to mixing with ligand π- or π*-orbitals. This is also connected with the extent of covalency in the metal–ligand σ-bond framework, but it is the π-framework where the effects of mixing can be more readily probed.

The occurrence of extensive metal dπ-ligand mixing is usually characterized by unexpectedly high energy "CT" bands that appear to have little CT character. This lack of CT character may be revealed by anomalies when electrochemistry–CT relationships (such as discussed below, Eq. (1)) are considered, and by narrow, intense electronic transitions that typically show enhancement of only one strong (metal–ligand stretching) vibration in the resonance Raman spectrum [2–4]. The CT bands arising from heavily mixed orbitals also show little solvatochromism. This last feature was discussed first by tom Dieck and co-workers as early as 1970 [33–35] where they dealt with the idea of a strong covalent interaction between a metal (Mo⁰) and a diimine ligand.

Recent work by Shin and co-workers [17–20] using the ZINDO method led to the suggestion that complexes containing Ru^{II} and protonated pyrazine, which were thought previously to show extensive mixing between one Ru d orbital and the pyrazine π orbital, in fact have a more modest amount of mixing and that the unexpectedly high energy band is raised in energy mainly by contributions from exchange energy terms.

We are interested to know what degree of mixing can cause the kind of "anomalous" behavior described above, and use the ZINDO method (modified INDO) as an aid to understanding these complexes. This method has been shown to give excellent predictions of trends in electronic transition energies and very good predictions of absolute band energies for visible region bands [7,36–42].

2. Methods

2.1. Geometry optimization

Structures of all complexes were obtained by using the modified INDO/1 semiempirical method (ZINDO/1) in the Hyperchem program (Hypercube Inc., Gainesville, FL, USA). The convergence condition was that the gradient was lower than 30 cal mol^{-1} $Å^{-1}$. The recommended value of the "resonance" integral parameter for Ru, $\beta(4d) = -26.5$ eV [43], overestimates the Ru–N bond strength and produces rather short Ru–N distances. To obtain better agreement with X-ray structural data for these complexes a value of $\beta(4d) = -20$ eV was used. All other parameters used in ZINDO/1 were the default parameters in the Hyperchem program.

2.2. Electronic spectra calculations

Electronic spectra calculations were performed using modified INDO/S (ZINDO/S), also in the Hyperchem program, as described by and utilizing the Ru INDO/S parameter set obtained by Krogh-Jespersen et al. [40]. Other atomic parameters were the default parameters of the Hyperchem program. For the abpy complexes the dihedral angle between the uncoordinated pyridine and the rest of the ligand was constrained to be 45° in agreement with crystal structure data [44].

Electronic spectra were calculated at the CIS level [45]. The number of configurations used was from ~800 to 1000 (e.g. approximately 20×20 to 21×23, occupied × unoccupied orbitals). Reasonable convergence of calculated transition energies in the visible region was achieved, i.e. increasing the number of configurations had little effect on the predicted visible region absorption energies. The overlap weighting factors σ–σ and π–π were set at 1.0 and 0.64 respectively [40]. Small variations in these parameter values had no substantive effect on the calculations except that closely spaced MO levels may change their relative positions. Oscillator strengths were calculated in the dipole length approximation including the one-center sp and pd atomic terms.

3. Results and discussion

3.1. Correlations between redox potentials and CT energies

Relationships between CT band energies and the related metal and ligand oxidation and reduction potentials have been discussed in depth [3,4,46–55] for ruthenium

and other complexes. In complexes containing an oxidizable metal, such as ruthenium(II), and a reducible ligand, the lowest energy intense transition is usually metal to ligand CT (MLCT). For the lowest energy spin-allowed MLCT transition the relationship between the optical transition energy and the first oxidation potential (E_{ox}, located primarily on the metal) and the first reduction potential (E_{red}, located primarily on the ligand) can be written [46,47]:

$$hv(\text{MLCT}) = E_{ox} - E_{red} + Q + \Delta\Delta G_s + \Delta(\text{sol}) + \chi_o + \chi_i \qquad (1)$$

where χ_o is the outer sphere or solvent reorganization energy and χ_i is the inner sphere or vibrational reorganization energy associated with the electronic transition. The difference, $E_{ox} - E_{red}$, is usually written as ΔE(redox), Q is the energy involved in transferring an electron from the (gas phase) reduced species to the oxidized species creating a ground state and an excited state molecule The term $\Delta\Delta G_s$ is $2\Delta G_s^{\circ} - \Delta G_s^{\circ +} - \Delta G_s^{\circ -}$, and $\Delta(\text{sol})$ is $\Delta G_s^{\circ *} - \Delta G_s^{\circ}$ where these terms are the standard free energies of solvation of the parent species, ΔG_s°, its oxidized (+) and reduced (−) and excited (*) analogs as identified. For these relationships to be valid the orbitals involved in the redox and CT processes should be the same and the redox potentials must be reversible. There should also be no significant effects from configuration interaction (CI) with higher states. For a large number of ruthenium diimine complexes the difference between hv(MLCT) and ΔE(redox) is ca 0.2 eV, i.e. the sum of Q (the various solvation terms), and χ_i is about 0.2 eV [50,56]. Q is probably negative.

Fig. 2 shows a plot of hv(MLCT) against ΔE(redox) for the three generic series to be discussed here, containing $[\text{Ru(bpy)}_{3-n}(\text{NN})_n]^{2+}$ where NN = bpz, abpy or bqdi, plus some other typical complexes (see Fig. 1 for legends). For complexes
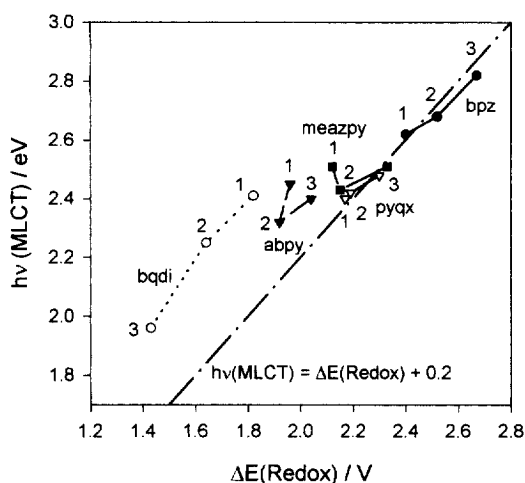

Fig. 2. The ΔE(redox) versus hv(MLCT) for series of $[\text{Ru(bpy)}_{3-n}(\text{NN})_n]^{2+}$ complexes with NN = 2,2′-azobipyridine (abpy), 2-(*m*-tolyl-azo)pyridine (meazpy), 2,2′-bipyrazine (bpz), pyridylquinoxaline (pyqx), and benzoquinonediimine (bqdi). CH$_3$CN, 298 K.

containing only bpy, bpz and pyqx (pyridylquinoxaline) the points for all three complexes lie on or close to the line of slope unity and the transition energies of the three complexes in the two generic series represented by these complexes lie in the order $n = 3 > n = 2 > n = 1$. As will be discussed below, this represents "normal" (i.e. easily explained using a simple model) behavior shown by a range of ruthenium diimine species [46–50].

In the abpy series the $n = 1$ species lies significantly away from the line and it has the highest energy MLCT band of the three (or five, with isomers) complexes. Similar behavior is also shown by other azopyridine complexes such as phenyl- and tolyl-azopyridine in analogous series containing bpy. In the abpy $n = 1$ case the difference between hv(MLCT) and ΔE(redox) is considerably larger than it is for complexes which fit the line (about 0.5 eV) and it is also higher (~ 0.4 eV) for the $n = 2$ and $n = 3$ species.

In the bqdi series the transition energies lie in the order $n = 1 > n = 2 > n = 3$, the reverse of the order for the "normal" complexes. Here, all three species lie above the line and have large differences (ca 0.6 eV) between hv(MLCT) and ΔE(redox). For the $[Ru(bpy)_2(NN)]^{2+}$ complexes where NN = abpy or bqdi or diaq [9] a second, weak CT band, v_2, (having clear CT character) can be observed to the low energy side of the main band, v_1 [2,57,58]. This provides some evidence that, at least in these species, the electrochemistry and CT processes do not involve the same orbitals. Table 1 shows differences between hv(MLCT) and ΔE(redox) for various complexes and also between v_1 and v_2 for some species.

An explanation of the two transitions has been given by various authors, but in the first instance by Magnuson and Taube [58]. The two transitions, v_1 and v_2 (Fig. 3), were assigned to transitions to the ligand π^* level from a split set of $d(t_{2g})$ orbitals, one of which was strongly stabilized by π back-bonding to the ligand, and gave rise to the strong v_1 band, and the other two of which were non-bonding with respect to the ligand π^* level of the strongly π-accepting ligand and gave rise to the weak near-infrared band, v_2. This explanation is also supported by recent work by Hupp and co-workers [67], Hush and co-workers [11–14], and Boxer and co-workers [15,16].

3.2. Zindo calculations

3.2.1. Geometry optimization

The ZINDO/1 method was used to obtain an optimized geometric structure for each complex. These structures were then used in the ZINDO/S method to obtain orbitals and predict electronic spectra, etc. The calculated Ru–N distances are in reasonable agreement with experimentally observed values [44,61,68,69] (see Appendix A, Table 8). Other bond distances and angles in the complexes were reproduced with average errors of 0.015 Å and 2° compared with X-ray structural data, where available. Constraining Ru–N distances to agree with experimental data, e.g. for $[Ru(bpy)_2(bqdi)]^{2+}$ or $[Ru(bpy)_3]^{2+}$, did not improve the calculated spectra significantly and made little difference to the character or energies of the valence orbitals. For example, a change in Ru–N distance from 2.04 to 2.06 Å in

Table 1
Comparison of ΔE(redox) and $h\nu$(MLCT)

Complex[a]	ΔE(redox) (V)	$h\nu$(MLCT) (eV)	Diff.[b]	$(\nu_1 - \nu_2)$[c]
$[Ru(bpz)_3]^{2+}$ [52–55]	2.67	2.82	0.15	
$[Ru(bpy)(bpz)_2]^{2+}$ [52–55]	2.52	2.68	0.16	
$[Ru(bpy)_2(bpz)]^{2+}$ [52–55]	2.40	2.62	0.22	
$[Ru(bqdi)_3]^{2+}$ [59,60]	1.42	1.89	0.47	
$[Ru(bpy)(bqdi)_2]^{2+}$ [61,60]	1.64	2.25	0.61	0.94
$[Ru(bpy)_2(bqdi)]^{2+}$ [3,4,61]	1.82	2.41	0.59	0.76
$[Ru(pyqx)_3]^{2+}$ [62]	2.30	2.48	0.18	
$[Ru(bpy)(pyqx)_2]^{2+}$ [62]	2.19	2.42	0.23	
$[Ru(bpy)_2(pyqx)]^{2+}$ [62]	2.17	2.40	0.23	
$[Ru(bpy)_2(diaq)]^{2+}$ [9]	1.45	2.2	0.75	0.84
$[Ru(meazpy)_3]^{2+}$ [63,64]	2.33	2.51	0.18	
$[Ru(bpy)(meazpy)_2]^{2+}$ [63,64]	2.15	2.43	0.28	
$[Ru(bpy)_2(meazpy)]^{2+}$ [63,64]	2.12	2.51	0.39	
$[Ru(abpy)_3]^{2+}$ [65,66] (mer)[d]	2.03	2.40	0.37	
$[Ru(bpy)(abpy)_2]^{2+}$ [65,66] (β)[d]	1.94	2.32	0.38	
$[Ru(bpy)_2(abpy)]^{2+}$ [65,66][d]	1.98	2.45	0.47	0.61

[a] Abbreviations: bpz = 2,2′-bipyrazineu; bqdi = benzoquinonediimine; pyrqx = 2,3-bis(2′-pyridyl)-quinoxaline; abpy = 2,2′-azobipyridine; meazpy = tolylazopyridine; diaq = 1,2-diimino-9,10-anthraquinone.

[b] $h\nu$(MLCT) $- \Delta E$(redox).

[c] The energy separation between the intense ν_1 transition and the HOMO→LUMO transition (ν_2).

[d] Unpublished data for $[Ru(bpy)_{3-n}(abpy)_n]^{2+}$ in acetonitrile versus SCE [65] are listed in the sequence: first oxidation, first reduction, second reduction, etc.: $n = 1$, $+1.638$, -0.343, -1.053, -1.688, -2.068 V; $n = 2$ (β), $+1.847$, -0.097, -0.557, -1.268, -1.583, -2.058, -2.198 V; $n = 3$ (mer), $+1.98$, -0.05, -0.39, -0.84, -1.30, -1.61, -1.86 V.
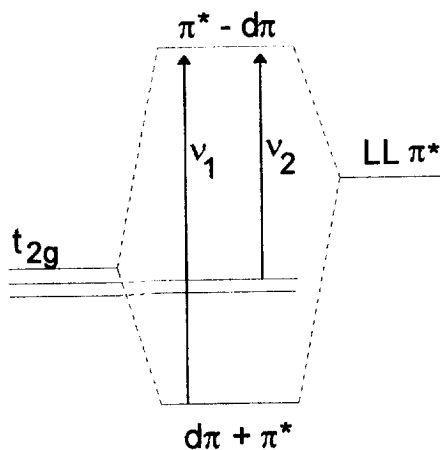

Fig. 3. Magnuson and Taube model showing one $d\pi$ orbital being stabilized relative to the other two t_{2g} orbitals by π-back-donation to the ligand π^* level.

$[Ru(bpy)_3]^{2+}$ (experimental: 2.056 Å [70]) produces only slight changes in MO eigenvalues (0.01–0.02 eV) and MO compositions (relative $\Delta \approx 2\%$).

3.2.2. Reliability of ZINDO/S

For calculation of electronic spectra we use the Krogh-Jespersen parameter set [40] for ruthenium which has been used in electronic structure calculations of many ruthenium complexes and has given reliable results. Our INDO/S results for $[Ru(bpy)_3]^{2+}$ (see Table 2) are comparable with, or better than, the DFT results recently reported by Daul et al. [70] or the ZINDO/S results reported by Broo and Lincoln [21]. With our systems, the Krogh–Jespersen parameter set appears to provide more accurate results, in terms of fitting the electronic spectra, than using the Ru parameters of Zerner and co-workers [10]. Further, the INDO/S model produces similar results to those of CASSCF/CASPT2 calculations for some first-row transition metal complexes studied [71].

For our complexes there is good agreement between calculated transition energies and observed electronic spectra in the visible and near-UV region (Table 3), although the calculated oscillator strengths usually overestimate the intensity of the MLCT bands by a factor of ~ 1.5–2. The agreement between the calculated transition energies and observed electronic spectrum in the UV region is less impressive, but the calculated spectra reproduce the general features of the experimental spectra. A more successful fit to the higher energy transitions probably requires a larger configurational interaction calculation. We conclude that the ZINDO model gives a good description of the electronic structure of these complexes.

3.2.3. Orbital electronic composition and electronic transition energies from ZINDO/S calculations

3.2.3.1. Orbital symmetries.
Comparisons of the composition of orbitals within a generic series are complicated by symmetry differences; the symmetry is D_3 for $[Ru(bpy)_3]^{2+}$, C_2 for the $n = 1$ and $n = 2$ complexes (in the bpz and bqdi series) and D_3 for $n = 3$. For the abpy series the symmetry is lower and there are several isomers to consider (see below). The three highest occupied orbitals are mainly Ru(4d)

Table 2
Comparison between ZINDO/S and DFT calculations for the molecular orbitals of $[Ru(bpy)_3]^{2+}$ (the D_3 point group) showing energies ($-\epsilon/eV$) and percentage ruthenium and bipyridine composition

Orbital	Γ	$-\epsilon$ (eV)	4d(Ru) (%)	bpy (%)
LUMO+1	e	6.07	6 (9)	94
LUMO	a_2	6.29	0 (0)	100
HOMO	a_1	12.44 (10.98)	79 (83)	20
HOMO−1	e	12.44 (11.30)	73 (73)	27
HOMO−2	e	14.15	1	99
HOMO−3	a_1	14.24	2	98

DFT data [70] in parentheses; Γ, irreducible representation.

orbitals which would be the t_{2g} set in octahedral complexes. Their symmetries are $a_1 + e$ in D_3, $a + e$ in C_3 and $2a + b$ in C_2. For $n = 1$, two of the t_{2g} set have π-symmetry and one has σ-symmetry with respect to the unique diimine ligand. Even though the symmetry is not O_h, this filled set is called Ru $d(t_{2g})$ here for convenience. Ru (dπ) is used where the specific π-characteristics are being discussed.

The three lowest unoccupied orbitals are ligand π* orbitals with symmetries $a_2 + e$ in D_3, $a + e$ in C_3 and $a + 2b$ in C_2 (Tables 4–6). In the D_3 point group, there is no mixing between the d orbitals and the LUMO, which has a_2 symmetry. In cases with formally lower symmetry than D_3, the LUMO has some contribution from d-orbitals but the situation is complicated by the fact that these complexes all contain an RuN_6 chromophore. In the bpz series the bpy and bpz ligands are sufficiently similar that the symmetry constraints of D_3 are not completely relaxed in the C_2 ($n = 1, 2$) species. Thus there is very little Ru(d) character (1.5%) in the LUMO of [Ru(bpy)$_2$(bpz)]$^{2+}$ even though it is largely a bpz-based orbital which lies significantly lower in energy than the mainly bpy LUMO + 1 and LUMO + 2 (Table 4). Elfring and Crosby [72] have discussed the effective symmetry of Ru complexes containing both bpy and phen (1,10-phenanthroline) and concluded that they should be regarded as D_3, though phen and bpy are more similar in their energies than any of the ligands discussed here.

It seems that the constraints of pseudo D_3 symmetry are completely relaxed in the azopyridine complexes because of the asymmetry of the abpy ligand—the pyridyl and azo nitrogen donor atoms are very different from each other. For bqdi it appears that the ligand is sufficiently different from bpy that the constraints of higher symmetry do not apply and for [Ru(bpy)$_2$(bqdi)]$^{2+}$ the d orbitals transform according to local C_{2v} symmetry rather than D_3.

Lying some 1–1.5 eV below the Ru(4d) levels is a set of ligand π orbitals which, in the $n = 3$ species, has the same symmetry as the d orbitals. These ligand orbitals are important, particularly in the bqdi complexes, because they mix strongly with Ru(4d) (see below).

3.2.3.2. Trends in orbital energies and mixing (Figs. 4–7). Molecular orbital diagrams for the various species under consideration here are shown in Figs. 4–6, and Fig. 7 displays pictorially the extent of mixing between metal d and ligand π and π* orbitals and between ligand orbitals for the $n = 1$ species. Since all the diimine ligands under consideration are reduced at a less negative potential than bpy, their π*-levels lie below those of bpy. Thus, subject to mixing, as discussed below, the LUMO of $n = 1$ and the LUMO and LUMO + 1 of $n = 2$ lie primarily on the non-bpy ligand. We are concerned with the detailed constitution of these low-lying diimine π* MOs, and also of the mainly metal-localized HOMO, HOMO − 1 and HOMO − 2 (t_{2g}) levels, and the highest filled π-levels of the diimine ligand.

However, there are a large number of MOs close to the frontier orbitals (a large state density) because of the large number of atoms in these molecules, and other, mainly lower energy, orbitals also contribute greatly to the bonding and charge distribution. For example, for [Ru(bqdi)$_3$]$^{2+}$ which has the lowest number of orbitals in this series of complexes the π-bonding between ruthenium and the bqdi ligands

Table 3

Calculated and observed spin singlet–singlet transition energies, oscillator strengths and assignments for $[Ru(LL)_n(bpy)_{3-n}]^{2+}$ species in the visible region (up to 25 000 cm^{-1}), INDO/S[a]

Complex	$h\nu_{obs}$ (log ϵ) 1000 cm^{-1}	$h\nu_{calc}$ 1000 cm^{-1}	f_{calc}	Assignment[b]
$[Ru(bpy)_3]^{2+}$	22.2 (4.15)	22.3	0.14	H−1→L (87)
	23.4 (4.08)	23.0	0.31	H−1→L+1 (64)
$[Ru(bpy)_2(bpz)]^{2+}$		19.9	0.002	H→L (89)
	21.1 (4.00)	21.9	0.19	H−2→L (86)
	24.2 (4.00)	23.5	0.09	H−1→L+1 (47); H→L+1 (30)
		24.2	0.11	H−2→L+3 (84)
$[Ru(bpy)(bpz)_2]^{2+}$	21.6 (4.08)	22.2	0.20	H−2→L (62); H−1→L+1 (28)
	24.1 (3.96)	23.8	0.15	H−2→L+1 (53); H−1→L+2 (24)
$[Ru(bpz)_3]^{2+}$	22.7 (4.11)	22.3	0.11	H−1→L (86)
	24.1 sh	23.4	0.27	H−1→L+1 (88)
$[Ru(bpy)_2(abpy)]^{2+}$		14.0	0.002	H→L (68)
	19.5 (3.76)	21.8	0.28	H−2→L (78)
	26.7 sh	24.4	0.13	H−1→L+1 (81)
α_1-$[Ru(bpy)(abpy)_2]^{2+}$	18.7 (3.98)	20.6	0.24	H−2→L (77)
	21.5 (3.79)	23.7	0.076	H−2→L+1 (52)
		25.0	0.19	no contribution > 18%
β-$[Ru(bpy)(abpy)_2]^{2+}$	18.8 (4.02)	20.8	0.25	H−2→L (59); H−1→L+1 (28)
	21.6 (3.76)	24.5	0.049	no contribution > 18%
		25.1	0.10	H−2→L+1 (37); H−1→L+2 (25)
fac-$[Ru(abpy)_3]^{2+}$	16.0 (2.70)	16.4	0.016	H→L (85)
	19.3 (4.00)	20.3	0.11	H−1→L (71)
	21.1 sh	22.6	0.39	H−1→L+1 (64)
mer-$[Ru(abpy)_3]^{2+}$		19.6	0.04	H−1→L+1 (36); H−1→L (27)
	19.6 (3.98)	21.1	0.12	H−2→L (59)
		22.1	0.12	H−2→L+2 (30); H−1→L+2 (26)
	21.1 sh	23.5	0.18	H−2→L+2 (52)
$[Ru(bpy)_2(bqdi)]^{2+}$		11.0	0.006	H→L (78)
	13.3 (2.74)(ν_2)			
		12.3	0.003	H−2→L (78)
	19.4 (4.30)	20.7	0.65	H−1→L (86)
	22.8 (3.84)	24.6	0.14	H−2→L+1 (75)
$[Ru(bpy)(bqdi)_2]^{2+}$	10.5 sh	8.5	0.011	H→L (86)
	15.4 sh	13.0	0.036	H−1→L (80)
	18.1 (4.42)	17.8	0.76	H−2→L (62); H−1→L+1 (28)
	22.1 (3.94)	22.0	0.057	H−3→L (73)
		23.1	0.10	H−5→L (58); H3→L+1 (24)

Table 3 (continued)

Complex	hv_{obs} (log ϵ) 1000 cm^{-1}	hv_{calc} 1000 cm^{-1}	f_{calc}	Assignment[b]
$[Ru(bqdi)_3]^{2+}$	15.2 (4.11)	15.5	0.30	H$-$1$\rightarrow$L (83)
	20.6 (4.36)	19.8	1.08	H$-$1$\rightarrow$L$+$1 (58)
	24.8 (3.67)	25.4	0.11	H$-$3$\rightarrow$L (59)

[a] Experimental data abstracted from Refs. [2,52,55,59,61,60,66,57]; H = HOMO; H $-$ 1 = HOMO $-$ 1, etc; L = LUMO, L $+$ 1 = LUMO $+$ 1; f is the oscillator strength; sh = shoulder. Calculated transitions with an oscillator strength less than about 0.01 are not included unless they relate to an observed experimental feature. Weak transitions which lie close to a reported strong transition and which would be obscured experimentally are also omitted.
[b] Percentage contribution of 1e$^-$ excitation to the excited state wavefunction in parentheses.

is not limited to the three low-lying π^* levels and the t_{2g} set. The sum of the Ru(4d) contributions in the aforementioned six levels accounts for approximately four electrons out of the expected six, i.e. about two "t_{2g}" electrons are distributed over the many other nearby MOs. In this particular case, as we discuss below, there is also strong mixing with the bqdi filled π-levels.

3.2.3.3. bpy. 2,2'-Bipyridine has been shown to be only a moderate π-acceptor by DFT calculations [70]. In $[Ru(bpy)_3]^{2+}$ there is no Ru contribution to the LUMO because of the constraints of D_3 symmetry, but there is calculated to be 9.5% Ru d character in each of the LUMO $+$ 1, $+$ 2e symmetry pair. Our ZINDO results give around 6.5% for the same orbitals. DFT results also show that there is as much bpy π character as there is π^* in the Ru(d) levels. The percentage mixing in the valence d orbitals calculated by the two methods is very similar.

3.2.3.4. bpz series (Fig. 4). There is a monotonic decrease in energy of the LUMO going from $n = 1$ to $n = 2$ to $n = 3$, but the calculated energy gap between the LUMO and the HOMO (or HOMO $-$ 2—they shift in parallel) increases from $n = 1$ to $n = 3$ due to the d orbitals being stabilized more than the bpz π^* (LUMO) level. The amount of mixing of the metal and ligand levels is quite small in the bpy–bpz complexes (Table 4). For all three species, the Ru(d) t_{2g}-derived orbitals are some 70–80% localized on the metal, and the bpz localized π^*-orbitals contain less than 10% Ru (d), whereas the bpy π^*-orbitals retain about 5–6% Ru(d) content.

An interesting result shown by the calculations is that there is substantial mixing of the ligand π levels; there is significantly more bpy character than there is Ru(d) character in the mainly bpz-based LUMO of $[Ru(bpy)_2(bpz)]^{2+}$, for example. This is in agreement with Elfring and Crosby's interpretation [72] of the Ru^{II} mixed ligand (bpy–phen) emission data and reflects the pseudo D_3 symmetry. There is also only a small amount of Ru(d) character in the ligand π levels in these complexes.

3.2.3.5. abpy series (Fig. 5). Experimental data are reported in the literature for two of the three possible $n = 2$ isomers (α and β; we assume here that the literature

Table 4
Frontier orbitals—irreducible representations, energies and percentage contribution of ruthenium d and diimine ligands: bpz

Orbital	$[Ru(bpy)_2(bpz)]^{2+}$					$[Ru(bpy)(bpz)_2]^{2+}$					$[Ru(bpz)_3]^{2+}$			
	Γ	$-\epsilon$ (eV)	4d (%)	bpz (%)	bpy (%)	Γ	$-\epsilon$ (eV)	4d (%)	bpz (%)	bpy (%)	Γ	$-\epsilon$ (eV)	4d (%)	bpz (%)
LUMO+2	a	6.29	6	2	92	b	6.53	5	8	88	e	7.00	8	92
LUMO+1	b	6.37	5	13	82	a	6.78	9	90	1	a$_2$	7.28	0	100
LUMO	b	6.71	3	79	17	b	7.00	2	91	7	a$_1$	13.44	78	22
HOMO	a	12.75	75	3	22	a	13.11	79	13	9	e	13.49	72	28
HOMO−1	a	12.79	77	9	14	b	13.11	72	14	13	e	14.66	1	99
HOMO−2	b	12.82	72	14	15	a	13.18	72	23	4	a$_1$	14.76	4	96
HOMO−3	a	14.28	1	87	13	b	14.46	1	99	0.4				
HOMO−4	b	14.34	1	0.3	99	a	14.49	1	66	33				
HOMO−5	a	14.42	2	12	86	a	14.60	3	32	66				

Table 5
Frontier orbitals— irreducible representations, energies and percentage contribution of ruthenium d and diimine ligands: abpy

Orbital	[Ru(abpy)(bpy)₂]²⁺				α₁-[Ru(abpy)₂(bpy)]²⁺					β-[Ru(abpy)₂(bpy)]²⁺				fac-[Ru(abpy)₃]²⁺				mer-Ru(abpy)₃²⁺		
	$-\epsilon$ (eV)	4d (%)	abpy (%)	bpy (%)	Γ	$-\epsilon$ (eV)	4d (%)	abpy (%)	bpy (%)	$-\epsilon$ (eV)	4d (%)	abpy (%)	bpy (%)	Γ	$-\epsilon$ (eV)	4d (%)	abpy (%)	$-\epsilon$ (eV)	4d (%)	abpy (%)
LUMO+2	6.20	6	0.4	94	b	6.24	6	4	91	6.30	5	3	91					6.86	16	84
LUMO+1	6.27	4	4	91	a	6.92	14	85	1	6.81	17	82	1	e	6.96	16	84	7.12	15	85
LUMO	6.88	11	81	8	b	7.13	7	87	6	7.21	6	91	6	a	7.34	3	97	7.41	2	98
HOMO	12.65	74	8	17	a	12.89	74	1.9	7	12.88	70	20	7	a	13.10	54	45	13.04	65	34
HOMO-1	12.76	74	7	19	b	12.96	60	26	14	13.10	68	19	14	e	13.41	53	47	13.37	56	43
HOMO-2	12.95	65	22	13	a	13.22	64	30	7	13.23	61	35	7	e	13.98	2	98	13.53	61	39
HOMO-3	14.03	2	94	4	b	14.10	0.3	99	6	14.03	1	97	6	a	14.12	15	85	13.95	1	99
HOMO-4	14.25	1	1	98	a	14.23	2	78	20	14.12	4	90	20					14.11	0	100
HOMO-5	14.29	2	3	96	a	14.32	4	17	79	14.31	3	10	79					14.24	9	91

Table 6
Frontier orbitals—irreducible representations, energies and percentage contribution of ruthenium d and diimine ligands: bqdi

	[Ru(bpy)₂(bqdi)]²⁺					[Ru(bpy)(bqdi)]²⁺					[Ru(bqdi)₃]²⁺ ᵇ			
	Γ [a]	$-\epsilon$ (eV)	4d (%)	bqdi (%)	bpy (%)	Γ	$-\epsilon$ (eV)	4d (%)	bqdi (%)	bpy (%)	Γ	$-\epsilon$ (eV)	4d (%)	bqdi (%)
LUMO+2	a	6.33	5	1	94	b	6.65	4	2	94	e	7.83	21	80
LUMO+1	b	6.44	5	3	93	a	7.80	27	71	2	a₂	8.61	0	100
LUMO	b	7.46	17	73	9	b	8.40	12	84	4	e	13.54	61	39
HOMO	a	12.87	68	20	12	a	13.26	55	42	3	e	13.77	51	49
HOMO−1	b	13.00	56	31	14	b	13.45	51	40	10	a₁	14.8	97	93
HOMO−2	a	13.00	73	3	23	a	13.68	51	40	9	a₁	15.27	22	78
HOMO−3	a	14.35	8	73	18	b	14.46	10	86	4				
HOMO−4	b	14.38	1	0	99	a	14.64	2	9	89				
HOMO−5	a	14.47	4	11	86	a	14.81	21	67	12				

[a] Irreducible representation.
[b] For "e" degenerate states the labeling in column 1 of single orbitals does not directly correspond.
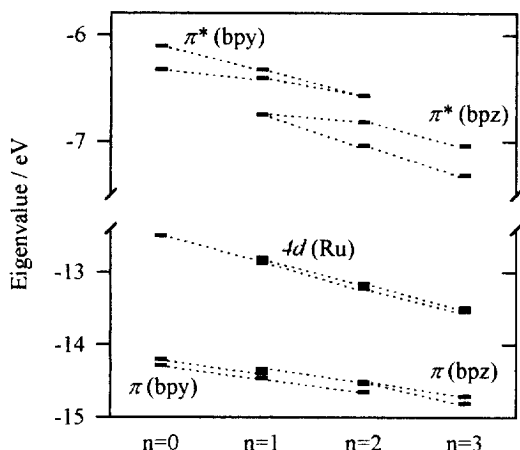
Fig. 4. The molecular orbital energies (eV) for $[Ru(bpy)_{3-n}(bpz)_n]^{2+}$ (INDO/S).

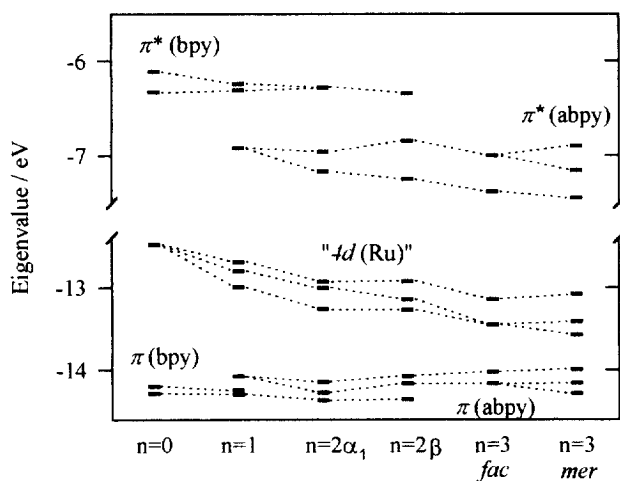Fig. 5. The molecular orbital energies (eV) for $[Ru(bpy)_{3-n}(abpy)_n]^{2+}$ (INDO/S).

assignment is correct, though it is somewhat uncertain) and for both the mer and fac $n=3$ isomers. Calculations for all five species are included in Table 5, but we will discuss only the lower symmetry species since $n=1$, β $n=2$, and mer $n=3$ all have C_1 symmetry, whereas α $n=2$ and fac $n=3$ have C_2 and C_3 symmetry respectively.

As in the bpz complexes, the valence orbitals all decrease in energy as bpy donors are replaced by abpy with the largest decreases being between the $n=1$ and $n=2$ species. The largest HOMO–LUMO gap is calculated for the $n=1$ complex, which coincidentally has the highest, both observed and calculated, transition energy (v_1). However, the HOMO $-$ 2–LUMO differences, which are related to the intense

MLCT v_1 band, vary little and trends depend upon which isomers are being considered.

Azobipyridine, like bipyrazine, is a poorer donor and a better π-acceptor than bpy, but more so as it is very easily reduced. Thus a greater degree of dπ–π* mixing is expected compared with the bpz series.

The changes in mainly Ru d(t_{2g}) and ligand π orbital energies when bpy is replaced by abpy are more pronounced than in the bpz case, though the trends are similar, with the HOMO being stabilized by about 0.2 eV per abpy (the HOMO−2 drops more per abpy, by ca 0.3 eV). The LUMO is stabilized by ~0.3 eV and then ~0.2 eV for $n=1$, to $n=2$ and $n=2$ to $n=3$ respectively. Species $n=2$ and $n=3$ may have less π-mixing with the LUMO because the d orbitals are relatively low in energy, due to abpy being a poorer donor than bpy. However, the maximum contribution of Ru(dπ) to the π*-levels of the ligand has increased, compared with bpz, to about 11–16% (Table 5). Indeed, the Ru d(t_{2g}) set is now only 50–65% localized on the metal, with the greatest mixing occurring in the $n=3$ species (especially the fac isomer).

Mixing of Ru (dπ) with the highest π levels of abpy and bpy is apparently not very important in this series of complexes, as in the case of bpz, though the amount of Ru in these levels is slightly more than in the bpz complexes. This is probably a result of the lowering of the ruthenium Ru d(t_{2g}) levels due to the good π-acceptor/weaker donor nature of abpy. The charge on Ru is calculated to be more positive than in the bpz complexes and the Ru d(t_{2g}) levels are closer to the π levels; consequently, mixing with them is increased.

3.2.3.6. bqdi series (Fig. 6).   It was previously proposed [1–4,7] that there is much greater mixing of Ru(dπ) and bqdi(π*) orbitals than between Ru(dπ) and bpy(π*) in [Ru(bpy)$_3$]$^{2+}$. These calculations agree with that observation. Indeed, in [Ru(bpy)$_{3-n}$(bqdi)$_n$]$^{2+}$ (π*) bqdi orbitals have Ru(4d) contributions from 12 to

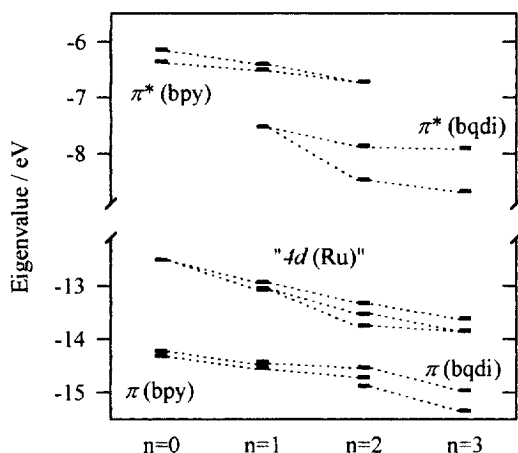Fig. 6. The molecular orbital energies (eV) for [Ru(bpy)$_{3-n}$(bqdi)$_n$]$^{2+}$ (INDO/S).

27% (except LUMO of $n = 3$ which is 0% for reasons of symmetry), whereas bpy(π^*) orbitals have Ru(4d) contributions ranging from 4.4 to 6.4%.

The bqdi free ligand has a low-lying empty π^* level of b_2 symmetry (C_{2v} point group, bqdi lies in the xz plane) and fairly high-lying filled π levels of a_2 and b_2 symmetry. Thus, of the Ru $d(t_{2g})$ set, one d orbital (b_2) is stabilized by interaction with the bqdi LUMO (π^*) but also destabilized by interaction with a lower filled b_2 π-orbital. The HOMO is the a_2 orbital destabilized by interaction with the filled bqdi a_2 π-orbital and the remaining Ru $d(t_{2g})$ orbital has σ-symmetry with respect to bqdi.

In the $n = 2$ species, symmetry C_2, there are π and π^* combinations from the two bqdi ligands of both a and b symmetry, so that any d orbital may interact with both. For $n = 3$, as in other D_3 symmetry complexes, the d orbital combinations ($a_1 + e$) can mix with p combinations of the same symmetry, whereas one d orbital (a_1) cannot interact with the p* levels which transform as $a_2 + e$.

Perhaps because bqdi is a good π-acceptor, the LUMO is relatively high in energy in the $n = 1$ complex as there is only one bqdi ligand to accept the available electron density and the two bpy ligands are relatively good donors, making the ruthenium fairly electron-rich. In this complex the LUMO contains 17% Ru character, compared with 12% and 0% in $n = 2$ and $n = 3$ respectively. However, the percentage Ru is not the only determining factor for the LUMO energy, because in $n = 2$ the LUMO is about 1 eV lower in energy than it is in $n = 1$, whereas for $n = 3$ the LUMO lies at almost the same energy as in $n = 2$, despite the differences in percentage Ru. This may be due to the charge on the Ru which is most positive in the $n = 2$ complex, rather than $n = 3$ as in the other generic series. This will tend to lower all the orbital energies and may be the reason for the $n = 2$ having an apparently anomalous LUMO energy. Ligand–ligand interactions, mediated through the metal, may also be important (see below).

The $n = 2$ and $n = 3$ species are, in fact, very similar in the degree of mixing and energies of orbitals. The Ru orbitals are highly mixed with both the bqdi π and π^* systems, resulting in the Ru $d(t_{2g})$ levels containing only around 50% Ru character for both $n = 2$ and $n = 3$, with the largest overall amount of mixing occurring for $n = 2$ (i.e. the lowest degree of Ru character in the mainly Ru $d(t_{2g})$ orbitals). For both $n = 2$ and $n = 3$ there are two bqdi *orbitals* (not ligands) available for π-acceptance because there is no d orbital of a_2 symmetry in the $n = 3$ complex to mix with the a_2 π^* combination, whereas all three d orbitals in both complexes can mix with a bqdi π combination.

The amount of mixing with the π levels increases as the Ru($d\pi$) levels are stabilized by π back-donation to bqdi and by replacement of bpy by bqdi (bpy seems to be a slightly stronger net donor). As the Ru($d\pi$) levels are stabilized they come closer to the set of π levels (a_2, b_2) in the free ligand, which has the same symmetry, and the closer these levels approach each other in energy the more they mix. This may be occurring more for $n = 3$ than for $n = 2$ as $n = 3$ has more total Ru character in the bqdi π levels than does $n = 2$, and the π-levels in $n = 3$ are lower in energy than would be expected by a simple extrapolation of $n = 1, 2$.

3.2.3.7. Ligand–ligand interactions (between equivalent ligands).   A remarkable observation is the comparatively large degree of ligand π^*-ligand π^*-coupling in some of these species (Figs. 4–6). Thus, in an $n=2$ or $n=3$ species, the π^*-orbital of a given ligand couples with that of another identical ligand to generate molecular orbitals whose coefficients span two or three ligand π^*-orbitals, thereby generating the LUMO, LUMO + 1, etc. of the complex, i.e. the a + b levels of $n=2$, and $a_2 + e$ levels of $n=3$. Ligand–ligand interaction could, in principle, be through space, or through $d\pi$–π^* mediation by the metal center. If the mixing with the metal ion and the ligand–ligand interaction were insignificant, then the a + b levels of $n=2$ would have the same energy, as would the $a_2 + e$ levels of $n=3$.

To investigate the possibility of direct through space ligand–ligand interactions (so-called ligand cluster model [73,74]), ZINDO calculations were performed on the three bqdi species *without* the Ru metal present, but with the same geometry as in the original calculation. The results show that the amount of interaction in the absence of the Ru atom is very small. For example, the difference in energy between the two bpy π^* orbitals in the $n=1$ species is 0.02 eV, compared with 0.11 in the metal complex. For both $n=2$ and $n=3$ the splitting between the bqdi(π^*) levels is 0.16 eV, which is a factor of 3–5 smaller than the splitting in the presence of the metal. Thus we conclude that direct ligand–ligand interaction is not very important and that large differences in π^* energies for two orbitals based on the same type of ligand in the same complex are due to interactions with different metal orbitals of appropriate symmetry, as well as to interactions with other ligand levels of the same symmetry.

The difference between π^* levels of the same type in the same complex increases between generic series in the order bpz < abpy < bqdi, i.e. in the same order as the degree of mixing. These differences are very large for bqdi, 0.6 eV and 0.78 eV for $n=2$ and $n=3$ respectively.

The comparative bonding picture is seen most vividly in Fig. 7, where for $n=1$ bqdi, compared with $n=1$ bpz and abpy, the metal contribution to the LUMO is clearly larger: mixing with ligand filled π-levels is greater (specifically HOMO − 3), and the HOMO, HOMO − 1 and HOMO − 2 d orbitals are clearly less pure.

This diagram also highlights the comparatively large intra-ligand mixing, between non-identical ligands, which is quite significant for all three systems, mediated by the central ruthenium atom. In species such as $[Ru(bpy)_2(LL)]^{2+}$ where LL is reduced prior to bpy, it is often assumed that the LUMO is pure LL. This is clearly a fairly crude approximation.

3.2.4. Predicted electronic transition energies

3.2.4.1. Agreement with experimental spectra.   The visible region spectra of most of the complexes are surprisingly simple given the number of possible transitions in these complexes, owing to the fact that most of the formally symmetry-allowed transitions are actually rather weak. We consider in detail the behavior of the lowest energy strong band in each complex. In most cases, this is calculated to be mainly due to a transition from the HOMO − 2 to the LUMO of the complex. Thus (all)
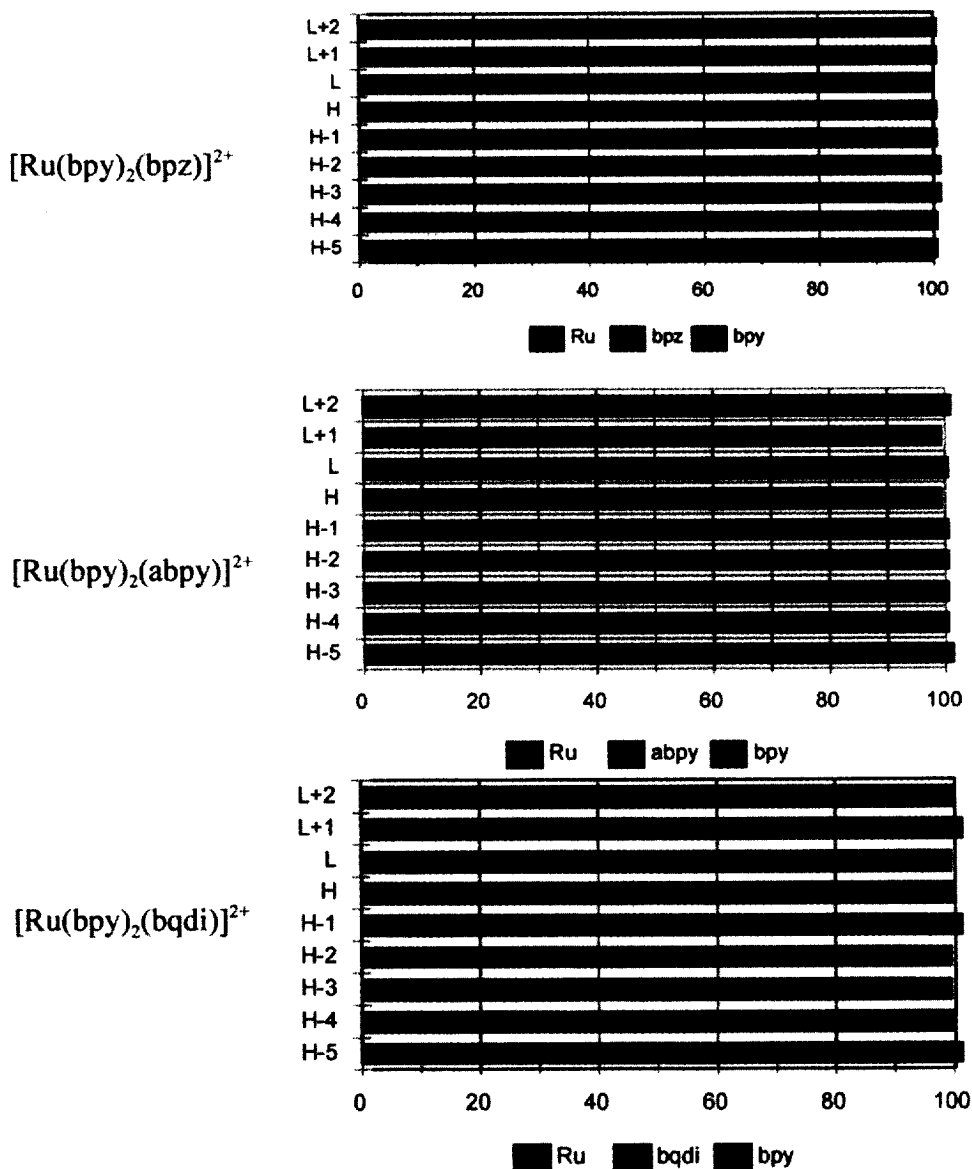
Fig. 7. A pictorial display of the extent of mixing in the frontier orbitals of $[Ru(bpy)_2(LL)]^{2+}$. The horizontal bars correspond to the orbitals as numerated in the left axis. The color codes define the sum of the squares of the molecular orbital coefficients of the total atomic contributions from metal, bipyridine and ligand LL as noted. In the case of the metal, the ruthenium contribution includes, in addition to Ru $d(t_{2g})$ contributions, very small s and p contributions so that the total sums to unity.

the relationships between hv(MLCT) and ΔE(redox) also contain a contribution from the d orbital splitting. This does not affect the quality of most of the earlier correlations because the splitting of the d orbitals is (apparently) very small in many of these systems and does not vary much amongst similar complexes. However, an extra term should be added to Eq. (1) to account for this.

Looking at the three series of complexes in more detail, we can analyze the trends in calculated and observed transition energies and relate them to the calculated energies of the valence orbitals. Depending on the complex, the main strong visible region band (Table 3) is HOMO-1, or HOMO$-2\rightarrow$LUMO and never, in these series of complexes, is it the HOMO$\rightarrow$LUMO. Thus the overall feature of the Magnuson–Taube analysis, that, in the $n=1$ species, the d-orbital involved in back-donation to the π-acceptor ligand, is stabilized relative to the others, is observed. However, it is not always the most stabilized, because underlying π-ligand levels of appropriate symmetry can "push up" the d levels, an effect not considered by Magnuson and Taube. Specifically, the intense transition v_1 in the $n=1$ species arises from the excitation $[Ru(d\pi)+\pi^*]\rightarrow[\pi^*-Ru(d\pi)]$ where $Ru(d\pi)$ is the specific $d\pi$ orbital which has the correct symmetry to interact with the ligand LUMO π^*-orbital.

We consider first how well the trends we observe in the ZINDO calculations for $n=1$–3 reproduce the observed spectroscopic or electrochemical features in the individual complexes.

3.2.4.2. bpz.   2,2'-Bipyrazine is a better π-acceptor and a poorer donor than bpy due to its lower energy (by 0.5 eV) π^* level and the presence of electron-withdrawing peripheral N atoms [75]. The trends in the electronic spectra can be predicted crudely from the changes in redox potentials in the series, or from E_L parameter theory [76], and they follow the trends in energy differences between relevant orbitals according to ZINDO. The redox potentials show that, as expected, the metal orbitals are stabilized as the number of bpz ligands increases, and that the bpz ligand π^* level is also stabilized due to the increased negative charge on the metal (i.e. by a secondary effect), but to a lesser extent. This would result in a blue shift of the MLCT transition from Ru to bpz in the series $n=1<n=2<n=3$. This is the trend observed and also predicted by the ZINDO/S calculations. The observed shift of the MLCT transition, Ru$\rightarrow$bpz, to the blue from $n=1$ to $n=3$, and that predicted by the shifts in redox potentials are similar in magnitude (ca 1600 cm^{-1}), whereas the ZINDO method calculates a smaller shift (ca 400 cm^{-1}) in the main MLCT band.

The lowest energy intense transitions are all mainly from the HOMO-2 to the LUMO, although in the $n=2$ complex there is strong mixing of states due to CI and a transition from HOMO-1 to LUMO$+1$ makes a significant contribution.

3.2.4.3. abpy. ΔE(redox) shows a minimum at $n=2$ in parallel with the observed (v_1) transition energies, largely because the first reduction potential for $n=1$ is unusually negative compared with $n=2,3$. The calculated band energies are all higher (by $\sim$2000 cm^{-1}) than the observed ones, but they tend to follow a similar trend with a maximum at $n=1$ and a minimum at $n=2$, though this last observation is isomer dependent.

3.2.4.4. bqdi. For the bqdi complexes, the magnitude of ΔE(redox) and the lowest energy intense electronic transition decrease monotonically in the order $n = 1 > n = 2 > n = 3$, the opposite behavior to that observed in the bpz and other generic series. The calculated transition energies also show this pattern; see further discussion below.

3.2.4.5. Low energy weak transitions. Considering first $n = 1$, as discussed above, only one dπ orbital has the correct symmetry to interact with the ligand LUMO π*, with excitation therefrom giving rise to the strong visible region transition, v_1. However, transitions, v_2, from the other two dπ orbitals to π* LUMO (one of which is always HOMO→LUMO in this series) can also be expected, but such transitions will be very weak due to poor ground-excited state overlap [3,4]. They are expected to occur to the red of the main visible region band, but are usually obscured by it except when they are displaced to very low energy [3,4]. The ZINDO analysis reveals that these bands are indeed well separated (to lower energy) from the main band in the $n = 1$ abpy and bqdi species where they have been observed experimentally (Table 3). However, in the $n = 2$ and $n = 3$ species there are several weaker spin-allowed transitions (HOMO and HOMO − 1, to LUMO and LUMO + 1) predicted to lie to the red of the main band causing a tail which, in some cases, e.g. $[Ru(bpy)(bqdi)_2]^{2+}$ shows some structure [61]. For bpz these weak transitions are all calculated to lie close to the main visible region band. As we develop in Section 3.3, the separation between these weak bands and the main absorption band increases with increasing π*-acceptor character of the ligand, i.e. with increasing Ru (dπ)–ligand (π*) mixing.

3.3. Coulombic and exchange contributions

The calculated energy separation between the weak HOMO→LUMO and the strong HOMO − 1 or 2→LUMO transition varies according to bpz $n = 1, 2, 3$ (2000, 2300, 1500 cm^{-1}), abpy ($n = 1$, $n = 2$ β, $n = 3$ mer) (7800, 6500, 6100 cm^{-1}) and bqdi $n = 1, 2, 3$ (9700, 9300, 4800 cm^{-1}). It is clearly larger for the abpy and bqdi species than for bpz. The overall splitting in the orbital energies of the Ru d(t_{2g}) sub-shell (Tables 4–6, Figs. 4–6), with maximum splitting 0.07 eV (ca 500 cm^{-1}) for bpz, 0.49 eV (ca 3950 cm^{-1}) for abpy (mer, $n = 3$) and 0.42 eV (3400 cm^{-1}) for bqdi, is clearly much smaller than any of the corresponding energy separations. As initially discussed by Shin and co-workers [17–20], the difference lies in varying coulombic (J) and exchange (K) contributions to these transitions.

Neglecting configurational interaction, the transition energies for these two transitions are given generally by [45]

$$\Psi_e \leftarrow \Psi_g = \epsilon_a - \epsilon_d - J_{ad} + 2K_{ad} \qquad (2)$$

where ϵ_a is the orbital energy of the LUMO and ϵ_d is the orbital energy of the donor orbital, HOMO, or HOMO − 1 or HOMO − 2 in this case. The quantity $(-J + 2K)$ is negative and usually quite large, so that the observed transition energy is signifi-

cantly less in energy than the HOMO–LUMO gap. In view of the comparative data discussed immediately above, it is evident that the $(-J+2K)$ term must be very different for the weak and for the strong transitions [17–20]. Table 7 lists these J and K energies as calculated by the ZINDO/S procedure.[1]

Owing to the extensive mixing between Ru $(d\pi)$ and π^* LUMO on the ligand, especially for bqdi and to a lesser degree abpy, the v_1 transition is more of a "vertical" RuNCCN ring transition than an MLCT transition, i.e. it is a transition between two orbitals which occupy largely the same region of space. There is, therefore, little net CT, as experimentally confirmed by the lack of solvatochromism in these species [3,4] and from electroabsorption spectroscopy experiments on related species showing relative little net electron transfer [16,18,19]. Thus the center of the charge distribution in the excited state is very close to that in the ground state, and K, which depends exponentially on the RuL separation [45], is large.

The separation between v_1 and v_2 and, in a related fashion, the unusual blue shift of v_1 (in some of the above $n = 1$ species) now becomes an indicator of extensive mixing, not solely because of the $d\pi$ splitting, though this may play a role, but because v_1 is shifted to the blue relative to v_2 by a larger K contribution.

This is seen very clearly in the data presented in Table 7, where consideration of the magnitudes of K and to a lesser degree J leads to a more detailed understanding of these generic series. For the v_1 transition K is small $(700\ \text{cm}^{-1})$ for $[\text{Ru(bpy)}_3]^{2+}$ and increases from bpz $(n = 1)$ to as large as $7200\ \text{cm}^{-1}$ for the highly coupled bqdi $n = 1$ species. This provides a qualitative view of our contention of increasing coupling from bpy < bpz < abpy < bqdi.

Table 7
Variation in $J_{d,L}$ and $K_{d,L}$ in the principal visible region (v_1) transition[a]

	n	$J_{d,L}$ (cm^{-1})	$K_{d,L}$ (cm^{-1})	$-J_{d,L}+2K_{d,L}$ (cm^{-1})
$[\text{Ru(bpy)}_3]^{2+}$	0	27 900	700	−26 500
$[\text{Ru(bpy)}_{3-n}(\text{bpz})_n]^{2+}$	1[b]	29 900	2100	−25 700
	2	29 200	1000	−27 200
	3	25 600	700	−24 200
$[\text{Ru(bpy)}_{3-n}(\text{bqdi})_n]^{2+}$	1[c]	36 200	7200	−21 800
	2	32 000	3800	−24 400
	3	29 700	2600	−24 500

[a] J and K data for the abpy series cannot be reliably extracted by the method used for bpz and bqdi because the low symmetry of the abpy complexes causes more extensive mixing.
[b] $[\text{Ru(bpy)}_2(\text{bpz})]^{2+}$ HOMO→LUMO (v_2), $K_{d,L} = 300$, $J_{d,L} = 28\ 500\ \text{cm}^{-1}$.
[c] $[\text{Ru(bpy)2(bqdi)}]^{2+}$ HOMO→LUMO (v_2), $K_{d,L} = 2000$, $J_{d,L} = 35\ 200\ \text{cm}^{-1}$.

[1] The J and K values were calculated according to the following general principles. One-electron excitation from a ground state (a^2, b^0) to (a^1, b^1) yields both a spin-singlet and a spin-triplet state. Their energy separation is simply $2K(a, b)$ [32,45]. Thus the ZINDO method was used to derive, for example, the HOMO→LUMO transition energy to both singlet and triplet states, with no CI; the energy difference is then taken as $2K(\text{HOMO}-\text{LUMO})$. Once K is known, Eq. (2) can be used to extract $J(a, b)$.

In the case of the HOMO→LUMO weak v_2 transition, the donor Ru (dπ) is not the same as that involved in coupling to the π^* ligand LUMO; so, there is a greater degree of charge redistribution, the charge in the excited state is spread over more of the ligand and K is small (Table 7). By the same argument, the coulombic term in the HOMO→LUMO transition is slightly smaller than in the HOMO-1, or HOMO-2→LUMO main transition, so that the term $(-J+2K)$ is significantly more negative (by approximately 10 000 cm^{-1} in the $n=1$ bqdi) in the v_2 transition. This is the primary contributor to shifting the [Ru (dπ)$+\pi^*$]→[$\pi^* -$Ru (dπ)] to the blue relative to the HOMO→LUMO transition even though the splitting of the dπ subset is fairly small.

Thus the difference in energy between the weak (v_2) and strong (v_1) bands is related to the degree of mixing, as suggested by Magnuson and Taube, but it is not a direct measure of it; rather, the difference in energy between v_1 and v_2 is related to the dπ splitting energy plus the difference in the value of $(-J+2K)$ for the two transitions, which difference increases with the degree of dπ/π^* LUMO mixing. Likewise, the difference between ΔE(redox) and hv(MLCT) is related to the same quantities, since in such circumstances hv(MLCT) is associated with v_1 not v_2.

The $n=1$ species are the only species in which the main transition occurs between the same two admixed orbitals. This is always the case for $n=1$, whereas for $n=2$ in C_2 the strong band is a mixture of a→b and b→a transitions, and for $n=3$ it is from e→a$_2$. This will affect the coulombic and exchange contributions: they will be larger in the excited state when the electron still occupies the same region of space, as with v_1 in the $n=1$ species. As Table 7 shows, the K contributions for $n=2$ and $n=3$ are rather smaller, implying a somewhat greater degree of CT.

4. Some final comments

We are now in a position to explain the reversed sequence of energies for $n=1, 2, 3$ for bqdi relative to the other diimines. Analysis of the calculated orbital energies allows one to understand this reversed behavior by taking into account the impact of Ru (dπ)–(π) bqdi, as well as the (π^*) bqdi interaction and its impact upon the magnitude of $(-J+2K)$. Thus, if we compare bpz with bqdi, in the former case the HOMO–LUMO separation is largest for $n=3$ whereas $(-J+2K)$ is the smallest; hence the hv(MLCT) is highest. However, for bqdi the HOMO–LUMO gap is largest and $(-J+2K)$ is smallest for $n=1$. Thus the ZINDO analysis is consistent with the experimental trends.

We can consider what the "correct" view of these complexes is from the standpoint of oxidation state. In terms of the percentage mixing in the LUMO, the bqdi $n=1$ species involves a net transfer of approximately 0.4 electrons to the bqdi by π back-donation. This is close to being formally Ru(2.5) bound to bqdi(0.5$-$). We also noted extensive mixing between filled metal dπ and ligand π-levels, especially important in all the bqdi species discussed here. This does not provide a mechanism to transfer net charge, but it does delocalize the electron density over both metal and

ligand. The complex then becomes more like an organic molecule, with several unsaturated components linked via the metal center.

It appears that only about 20% mixing of the d orbitals into the ligand acceptor levels is necessary to give some anomalous effects in spectra and electrochemistry. As far as mixing with π^* levels is concerned, the three generic series show clear differences, with the average amount of Ru in LL (π^*) being surprisingly consistent for a given ligand, i.e. 3–5% for bpz, 10% for abpy and $\sim 17\%$ for bqdi.

π back-donation (mixing) also reveals itself in an interesting fashion by mediating the coupling between the π^* levels of the several identical ligands in the $n = 2, 3$ species, causing a separation of the several representations increasing with the extent of back-donation.

Acknowledgements

Appendix A

Table 8 lists the characteristic Ru–N bond distances obtained with the ZINDO/1 optimization, compared with experimental X-ray distance where available.

Table 8
Ru–N internuclear distances obtained by INDO/1 geometry optimization [43]

Complex	d(Ru–N(bpy)) (Å)[a]	d(Ru–N(L)) (Å)[a]
$[Ru(bpy)_2]^{2+}$	2.04 (2.06 [68,69])	
$[Ru(bpy)_2(bqdi)]^{2+}$	2.03 (2.06–2.09 [61])	2.04 (2.00–2.04 [61])
$[Ru(bpy)(bqdi)_2]^{2+}$	2.02–2.03	2.02
$[Ru(bqdi)_3]^{2+}$	—	2.03
$[Ru(bpy)_2(bpz)]^{2+}$	2.04	2.04
$[Ru(bpy)(bpz)_2]^{2+}$	2.04	2.04
$[Ru(bpz)_3]^{2+}$	—	2.04 (2.05 [68,69])
$[Ru(bpy)_2(abpy)]^{2+}$	2.03–2.04	2.04
α_1-$[Ru(bpy)(abpy)_2]^{2+}$ [b]	2.04	2.03
β-$[Ru(bpy)(abpy)_2]^{2+}$ [b]	2.03	2.03–2.04
fac-$[Ru(abpy)_3]^{2+}$	—	2.02
mer-$[Ru(abpy)_3]^{2+}$	—	2.03–2.04 (2.04–2.07 [44])

[a] Experimental X-ray data (with reference) in parentheses.

[b] Notation as in Ref. [66].

References

[1] H. Masui, P.R. Auburn, A.B.P. Lever, Inorg. Chem. 30 (1991) 2402.

[2] H. Masui, A.B.P. Lever, E.S. Dodsworth, Inorg. Chem. 32 (1993) 258.

[3] A.B.P. Lever, H. Masui, R.A. Metcalfe, D.J. Stufkens, E.S. Dodsworth, P.R. Auburn, Coord. Chem. Rev. 125 (1993) 317.

[4] D.J. Stufkens, Th.L. Snoeck, A.B.P. Lever, Inorg. Chem. 27 (1988) 953.

[5] M. Haga, E.S. Dodsworth, A.B.P. Lever, Inorg. Chem. 25 (1986) 447.

[6] A.B.P. Lever, P. Auburn, E.S. Dodsworth, M. Haga, M. Melnik, W.A. Nevin, J. Am. Chem. Soc. 110 (1988) 8076.

[7] R.A. Metcalfe, A.B.P. Lever, Inorg. Chem. 36 (1997) 4762.

[8] P.R. Auburn, E.S. Dodsworth, M. Haga, W. Liu, W.A. Nevin, A.B.P. Lever, Inorg. Chem. 31 (1991) 3502.

[9] C.J. da Cunha, S.S. Fielder, D.V. Stynes, H. Masui, P.R. Auburn, A.B.P. Lever, Inorg. Chim. Acta 242 (1996) 293.

[10] K.K. Stavrev, M.C. Zerner, T.J. Meyer, J. Am. Chem. Soc. 117 (1995) 8684.

[11] J. Zeng, N.S. Hush, J.R. Reimers, J. Am. Chem. Soc. 118 (1996) 2059.

[12] J. Zeng, N.S. Hush, J.R. Reimers, J. Phys. Chem. 100 (1996) 19292.

[13] J. Zeng, N.S. Hush, J.R. Reimers, J. Phys. Chem. 99 (1995) 10459.

[14] J. Zeng, N.S. Hush, J.R. Reimers, J. Am. Chem. Soc. 118 (1996) 2059.

[15] S.G. Boxer, R.A. Goldstein, D.J. Lockhart, T.R. Middendorf, L. Takiff, J. Phys. Chem. 93 (1989) 8280.

[16] D.H. Oh, M. Sano, S.G. Boxer, J. Am. Chem. Soc. 113 (1991) 6880.

[17] Y.G.K. Shin, B.S. Brunschwig, C. Creutz, M.D. Newton, N. Sutin, J. Phys. Chem. 100 (1996) 1104.

[18] Y.K. Shin, B.S. Brunschwig, C. Creutz, N. Sutin, J. Phys. Chem. 100 (1996) 8157.

[19] Y.K. Shin, B.S. Brunschwig, C. Creutz, N. Sutin, J. Am. Chem. Soc. 117 (1995) 8668.

[20] Y.K. Shin, D.J. Szalda, B.S. Brunschwig, C. Creutz, N. Sutin, Inorg. Chem. 36 (1997) 3190.

[21] A. Broo, P. Lincoln, Inorg. Chem. 36 (1997) 2544.

[22] O.V. Sizova, V.I. Baranovskii, N.V. Ivanova, A.I. Panin, Int. J. Quant. Chem. 65 (1997) 183.

[23] O.V. Sizova, V.I. Baranovskii, N.V. Ivanova, A.I. Panin, J. Struct. Chem. 37 (1996) 525.

[24] O.V. Sizova, N.V. Ivanova, V.I. Baranovskii, A.B. Nikolskii, Russ. J. Struct. Chem. 35 (1994) 12.

[25] O.V. Sizova, N.V. Ivanova, V.I. Baranovskii, A.B. Nikolskii, A.Yu. Timoshkin, Koord. Khim. 21 (1995) 47.

[26] O.V. Sizova, N.V. Ivanova, V.I. Baranovskii, A.I. Panin, Koord. Khim. 22 (1996) 591.

[27] K.J. LaChance-Galang, P.E. Doan, M.J. Clark, U. Rao, A. Yamano, B.M. Hoffman, J. Am. Chem. Soc. 117 (1995) 3529.

[28] E.C. Constable, C.E. Housecroft, Polyhedron 9 (1990) 1939.

[29] M.-A. Haga, T. Matsumura-Inoue, K. Shimizu, G.P. Sata, J. Chem. Soc. Dalton Trans. (1989) 371.

[30] J.A. Crayston, D.C. Cupertino, T.J. Dines, J. Chem. Soc. Dalton Trans. (1991) 1603.

[31] J.A. Crayston, D.C. Cupertino, H.S. Forster, Synth. Met. 35 (1990) 365.

[32] A.B.P. Lever, Inorganic Electronic Spectroscopy, 2nd edition, Amsterdam, Elsevier, 1984.

[33] H. Friedel, I.W. Renk, H. Tom Dieck, J. Organomet. Chem. 26 (1971) 247.

[34] H. Tom Dieck, I.W. Renk, Angew. Chem. 9 (1970) 793.

[35] H. Tom Dieck, I.W. Renk, Chem. Ber. 104 (1971) 110.

[36] J. Ridley, M.C. Zerner, Theor. Chim. Acta 32 (1973) 111.

[37] J. Ridley, M.C. Zerner, Theor. Chim. Acta 42 (1976) 223.

[38] M.C. Zerner, G.H. Loew, R.F. Kirchner, U.T. Mueller-Westerhoff, J. Am. Chem. Soc. 102 (1980) 589.

[39] W.P. Anderson, W.D. Edwards, M.C. Zerner, Inorg. Chem. 25 (1986) 2728.

[40] K. Krogh-Jespersen, J.D. Westbrook, J.A. Potenza, H.J. Schugar, J. Am. Chem. Soc. 109 (1987) 7025.

[41] K. Krogh-Jespersen, X. Zhang, J.D. Westbrook, R. Fikar, K. Nayak, W.-L. Kwik, J.A. Potenza, H.J. Schugar, J. Am. Chem. Soc. 111 (1989) 4082.

[42] K. Krogh-Jespersen, X. Zhang, Y. Ding, J.D. Westbrook, J.A. Potenza, H.J. Schugar, J. Am. Chem. Soc. 114 (1992) 4345.

[43] W.P. Anderson, T.R. Cundari, M.C. Zerner, Int. J. Quant. Chem. 39 (1991) 31.
[44] J. Fees, H.-D. Hausen, W. Kaim, Z. Naturforsch. Teil B: 50 (1995) 15.
[45] A. Szabo, N.S. Ostlund, Modern Quantum Chemistry, Macmillan, New York, 1982.
[46] E.S. Dodsworth, A.B.P. Lever, Chem. Phys. Lett. 112 (1984) 567.
[47] E.S. Dodsworth, A.B.P. Lever, Erratum, Chem. Phys. Lett. 116 (1985) 245.
[48] E.S. Dodsworth, A.B.P. Lever, Chem. Phys. Lett. 119 (1985) 61.
[49] E.S. Dodsworth, A.B.P. Lever, Erratum, Chem. Phys Lett. 122 (1985) 420.
[50] E.S. Dodsworth, A.B.P. Lever, Chem. Phys. Lett. 124 (1986) 152.
[51] G.A. Neyhart, J.T. Hupp, J.C. Curtis, C.J. Timpson, T.J. Meyer, J. Am. Chem. Soc. 118 (1996) 3724.
[52] D.P. Rillema, G. Allen, T.J. Meyer, D. Conrad, Inorg. Chem. 22 (1983) 1617.
[53] T.J. Meyer, Inorg. Chem. 26 (1987) 2332.
[54] H.B. Ross, M. Boldajii, D.P. Rillema, C.B. Blanton, R.P. White, Inorg. Chem. 28 (1989) 1013.
[55] Y. Ohsawa, K.W. Hanck, M.K. DeArmond, J. Electroanal. Chem. 175 (1984) 229.
[56] A.B.P. Lever, Can. J. Anal. Sci. Spectrosc. 42 (1997) 24.
[57] W. Kaim, personal communication, 1997.
[58] R.H. Magnuson, H. Taube, J. Am. Chem. Soc. 97 (1975) 5129.
[59] L.F. Warren, Inorg. Chem. 16 (1977) 2814.
[60] M. Ebadi, A.B.P. Lever, unpublished results.
[61] P. Belser, A. Zelewsky, M. Zehnder, Inorg. Chem. 20 (1981) 3098.
[62] D.P. Rillema, D.G. Taghdiri, D.S. Jones, C.D. Keller, L.A. Worl, T.J. Meyer, H.A. Levy, Inorg. Chem. 26 (1987) 578.
[63] S. Goswami, R. Mukherjee, A. Chakravorty, Inorg. Chem. 22 (1983) 2825.
[64] S. Goswami, A.R. Chakravarty, A. Chakravorty, Inorg. Chem. 20 (1981) 2246.
[65] E.S. Dodsworth, A.B.P. Lever, unpublished results.
[66] M. Krejcik, S. Zalis, J. Klima, D. Sykora, W. Matheis, A. Klein, W. Kaim, Inorg. Chem. 32 (1993) 3362.
[67] L. Karki, H.P. Lu, J.T. Hupp, J. Phys. Chem. 100 (1996) 15637.
[68] H. Lai, D.S. Jones, D.C. Schwind, D.P. Rillema, J. Crystallogr. Spectrosc. Res. 20 (1990) 321.
[69] D.P. Rillema, D.S. Jones, C. Woods, H.A. Levy, Inorg. Chem. 31 (1992) 2935.
[70] C. Daul, E.J. Baerends, P. Vernooijs, Inorg. Chem. 33 (1994) 3538.
[71] B.O. Roos, K. Andersson, M.P. Fulscher, P.-A. Malmqvist, L. Serrano-Andres, K. Pierloot, M. Merchan, Adv. Chem. Phys. 93 (1996) 219.
[72] W.H. Elfring Jr.,, G.A. Crosby, J. Am. Chem. Soc. 103 (1981) 2683.
[73] A.A. Vlcek, Coord. Chem. Rev. 43 (1982) 39.
[74] S. Zalis, M. Krejcik, V. Drchal, A.A. Vlcek, Inorg. Chem. 34 (1995) 6008.
[75] R.J. Crutchley, A.B.P. Lever, Inorg. Chem. 21 (1982) 2276.
[76] A.B.P. Lever, Inorg. Chem. 29 (1990) 12715.